ISSN: 2615-9740

JOURNAL OF TECHNICAL EDUCATION SCIENCE
Ho Chi Minh City University of Technology and Education
Website: https://jte.edu.vn
Email: jte@hcmute.edu.vn

Crystallization of Potassium Dihydrogen Phosphate Considering Particle Size Evolution

Tam Minh Le[1*], Phuong Bui Thi Thanh[2], Tuyen Kha Chan[2]
[1]*Ho Chi Minh City University of Technology and Education, Vietnam*
[2]*Nong Lam University, Ho Chi Minh City, Vietnam*

[*]Corresponding author. *Email:* tamlm@hcmute.edu.vn

ARTICLE INFO

Received:	27/12/2024
Revised:	14/03/2025
Accepted:	04/04/2025
Published:	28/05/2025

KEYWORDS

KDP;

Solid-liquid equilibrium;

Meta stable zone width;

Crystallization;

Antisolvent.

ABSTRACT

Potassium dihydrogen phosphate (KDP) is widely utilized in food additives, laser technology, and multi-nutrient fertilizers. Besides the purity, particle size distribution (PSD) of KDP is critical quality parameter, which is the primary focus in this study. For this purpose, a systematic study was carried out. KDP crystals were synthesized through a crystallization process employing various operation modes. The evolution of crystal size over time was monitored using two distinct techniques, including real-time online monitoring via laser measurement and offline analysis through microscopic analysis. The crystal growth dynamics were found to be influenced by the degree of supercooling and the anti-solvent employed. Crystals obtained through natural cooling versus anti-solvent technique exhibited that nucleation and crystal growth are strongly dependent on fluctuations in supersaturation levels. Chemical composition analysis of the optimized products revealed that the KDP crystals achieved a purity greater than 99%, confirming that the crystallization process was efficient, with minimal incorporation of impurities into the crystal structure, thereby ensuring the product's quality.

Doi: https://doi.org/10.54644/jte.2025.1753

1. Introduction

KDP (Potassium Dihydrogen Phosphate – KH_2PO_4) is a compound with numerous important applications across various fields. In the food industry, KDP is used as a food additive to regulate pH levels, stabilize products, and provide a source of phosphate during food processing. Thanks to its high safety and efficiency, KDP plays a crucial role in enhancing food quality and extending shelf life. [1], [2]

Additionally, KDP is well-known in the field of nonlinear optical (NLO) materials. With its ability to generate optical effects such as frequency mixing and frequency doubling, KDP is widely applied in the manufacturing of laser devices, telescopes, and advanced optical systems. Notably, this material is highly valued for its excellent mechanical durability, high optical transparency, and stable thermal properties, contributing to the improved performance of modern optical devices. [3]-[7]

The large-scale production of KDP is typically achieved through crystallization processes which are normally contaminated with NaDP due to the similarity of K^+ and Na^+ ions. Research in this area focuses on the variation of supersaturation levels in the liquid phase, which allows the prediction of the solid-phase mass based on the principle of mass conservation. However, information about the solid phase is not solely limited to its total mass but also significantly depends on its properties, such as phase form, polymorph type, crystalline hydrates, purity, morphology and particle size distribution (PSD). Among these factors, PSD holds importance comparable to purity due to its critical role in various applications. For instance, in pharmaceutical granulation processes, particle size can directly influence dissolution rates and other functional properties, making PSD a key parameter for optimizing the material's performance in specific applications. [8], [9]

Many studies have demonstrated that alcohol acts as an antisolvent in the KDP-water system. According to Le et al., the addition of C_1-C_4 alcohols significantly reduces the solubility of KDP in water [10]. Similar results were also reported by Barata et al. [11]. This finding confirms the role of alcohols as antisolvents, and in this study, ethanol was selected due to it nontoxicity and popularity.

KDP crystals belong to a tetragonal crystal system The unit cell parameters are a = b = 0.7453 nm, c = 0.6975 nm, and Z = 4 [12]. However, different crystallization conditions can lead to varying growth rates of different crystal faces, thereby influencing the resulting morphology. Depending on the crystallization conditions, KDP can be obtained in prismatic, needle-like, or other morphological forms. However, the basic structure of KDP can be seen in Figure 1.

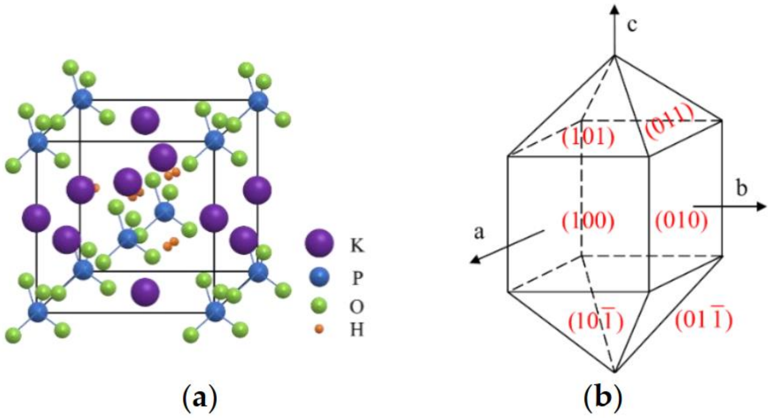

Figure 1. *KDP crystal structure [12]*

The principle of the crystallization process is illustrated in Figure 2 [13]. The boundaries of the metastable zone width (MSZW) and the solubility curve define the operational region for crystallization. When the system reaches an excessively high level of supersaturation, crystallization enters an uncontrollable regime due to an accelerated crystallization rate. Conversely, if the system falls below the solubility curve, crystallization does not occur. Therefore, it is very important to precisely detect controllable regime for crystallization process operation.

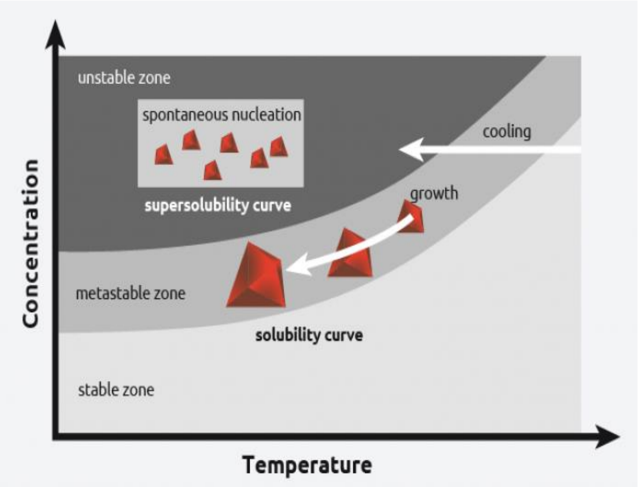

Figure 2. *Principle of crystallization process [13]*

The objective of this study is to systematically investigate the solid-liquid equilibrium of the KDP-water system (contaminated with NaDP) in the presence and absence of ethanol. Additionally, the metastable zone width (MSZW) is determined by lowering the temperature and analyzing the nucleation process. Based on the obtained thermodynamic and kinetic data, crystallization processes are designed, focusing on the effects of varying supersaturation levels at different temperatures. Particularly, antisolvent crystallization technique is studied and compared with cooling crystallization. All crystallization processes are carefully monitored by tracking changes in the liquid-phase concentration, while the corresponding solid-phase properties, including particle size variations, are analyzed using microscopy and in-situ monitoring laser based technique for large populations.

2. Experimental method

2.1. Chemicals

KDP was purchased from Xilong Scientific Co. with a purity of 99.5% and purity of $NaDP.2H_2O$ at analytical reagent level. Water used in this study was double distilled water. Ethanol (>97%) from Merck was used.

2.2. Solubility Determination Method

The solubility measurements were conducted using a polythermal method with the C1 apparatus (Figure 3) [14]-[16]. The principle of this device is based on real-time laser monitoring of turbidity changes in the sample under increasing temperature programs. In this study, a slow heating rate of 0.5 K/min was employed. Pre-prepared suspensions with known concentrations were gradually dissolved, and the temperature at which complete dissolution occurred was identified as the saturation temperature (T_{sat}).

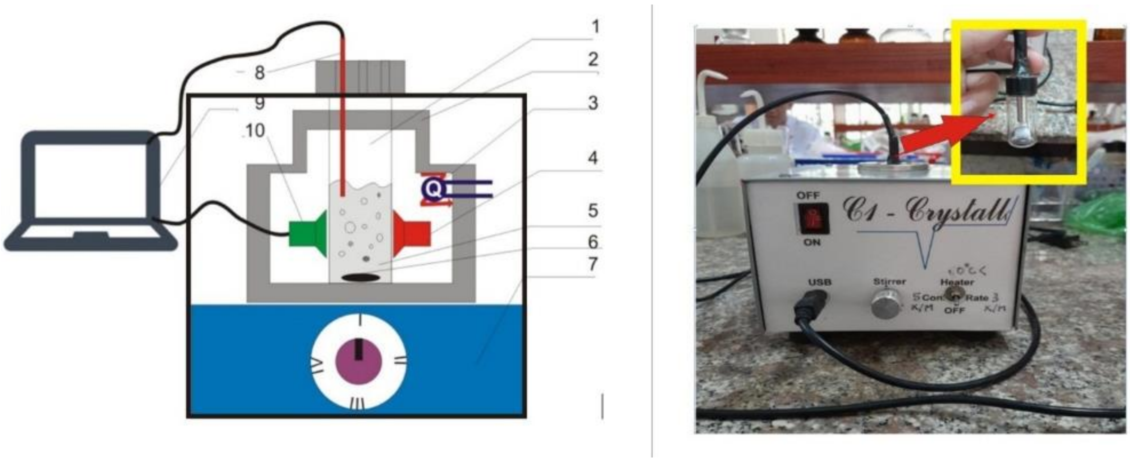

Figure 3. *Principle structure of C1 equipment (left) and prototype (right). The main components conceptually include (1) a glass vial, (2) a thermal insulation chamber, (3) a temperature control unit, (4) a laser source, (5) a studied sample, (6) a magnetic bar, (7) a magnetic stirrer, (8) a temperature sensor, (9) a computer, and (10) a laser receiver. [14]-[16]*

2.3. Method for Determining the Metastable Zone Width (MSZW)

The metastable zone width was also determined using the C1 apparatus through a controlled cooling process. During cooling down, the solution was gradually supersaturated until spontaneous nucleation occurred. This point, referred to as the “cloud point”, corresponds to the nucleation temperature (T_{nuc}). Herein, a cooling rate of 1 $^{o}C.min^{-1}$ was applied. Procedure was according to description of Nývlt. [9]

2.4. Crystallization Experiments

Three crystallization modes were conducted to compare the effects of supersaturation and the role of the antisolvent. The starting solution was saturated at 55^{o}C containing 10% (w/w) NaDP. The product purity was analyzed via EDS method. In the preliminary test, three samples was independently checked via EDS analysis that resulted in less than 0.6% purity deviation between these samples. The crystallization was conducted via isothermal auto-seeded technique [17]. Three operation modes were performed including:

- Mode #1. Cooling the saturated solution from 55°C to 35°C.
- Mode #2. Cooling the saturated solution from 55°C to 45°C.
- Mode #3. Adding 5% ethanol as an antisolvent to the saturated solution.

3. Results and Discussion

3.1. XRD analysis

In Figure 4, the XRD analysis of the structure reveals that KDP (potassium dihydrogen phosphate) crystallizes in a crystal form consistent with its standard diffraction pattern. Figure 4a presents the reference pattern of KDP while Figures 4b and 4c correspond to material crystallized from water and mixture of water/ethanol. Indeed, these three XRD patterns are identical which indicates that the applied experimental conditions were suitable for the formation of pure KDP crystals, free from contamination by other polymorphic forms. Consequently, it can be concluded that the presence of ethanol in the experimental setup does not have any significant effect on the crystalline phase structure of KDP.

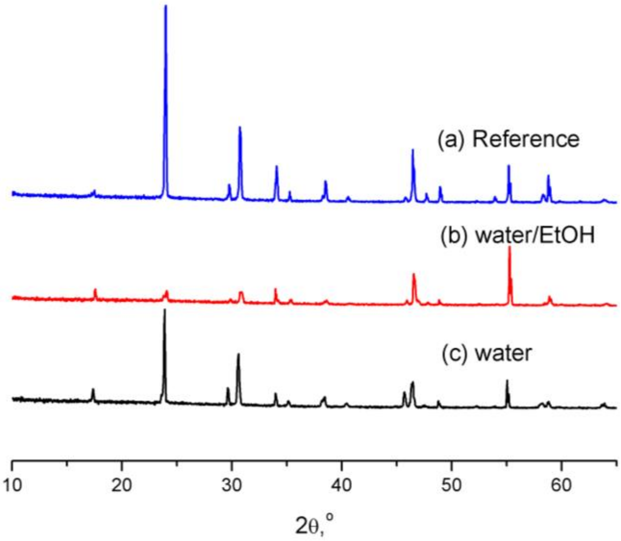

Figure 4. *XRD analyses*

3.2. SEM analysis

Although XRD confirms that the crystalline solid phase remains unaffected, further studies on the morphology of the crystals are still necessary. The morphology of KDP crystals grown under two different conditions, with and without ethanol, was analyzed using SEM (Scanning Electron Microscopy). Figure 5 presents representative crystals for both types of samples.

In Figure 5a, KDP crystals slowly grown in an aqueous solvent exhibit a prismatic shape with two ends forming regular quadrangular pyramids, and the crystal faces show relatively uniform growth rates. Under fast cooling, smaller crystals were obtained as seen in Figure 5b. Especially, the presence of ethanol causes significant changes in the growth rates of the crystal faces, as depicted in Figure 5c. The interaction between water and ethanol as solvent components leads to preferential growth along the (100) and (010) planes, resulting in crystals with a length significantly exceeding their width. The shape differences between the crystals in Figures 5a, b, c provide clear evidence supporting this observation.

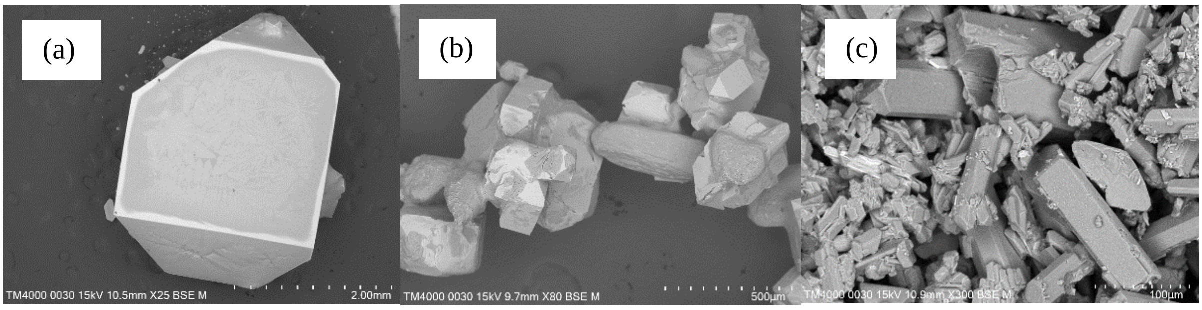

Figure 5. *Scanning electron microscope analysis for (a) slow; (b) fast cooling; (c) antisolvent crystallization*

3.3. SLE and MSZW determination

The solubility of KDP was determined using the polythermal method, and the results are illustrated in Figure 6. The findings indicate that KDP has relatively high solubility in water, with its weight percentage reaching approximately 25% at 40°C. Overall, the solubility curve aligns well with the data published by Barata et al. [11].

The high solubility of KDP can be attributed to its effective solvation process. Water, as a strongly polar solvent, interacts efficiently K^+ and $H_2PO_4^-$ ions, enhancing the solubility of KDP. Additionally, the solubility of KDP increases with temperature due to the endothermic nature of the dissolution process, which is consistent with the concepts reported by Bromley et al. [18]

Figure 6b illustrates the role of ethanol as an antisolvent, demonstrating that the addition of a small amount (5% V/V) of ethanol immediately reduces the solubility of KDP by 20%. However, the slope of the solubility curve remains similar to the case where only water is present. This reduction in solubility is related to changes in the solvent's properties. Ethanol, being less polar than water, decreases the overall polarity of the solvent mixture when introduced. As a result, the solvation efficiency for K^+ and $H_2PO_4^-$ ions is reduced, leading to decreased solubility. In short, ethanol acts as an antisolvent in the KDP liquid solution system, altering the solvent environment and reducing the solubility of KDP [10].

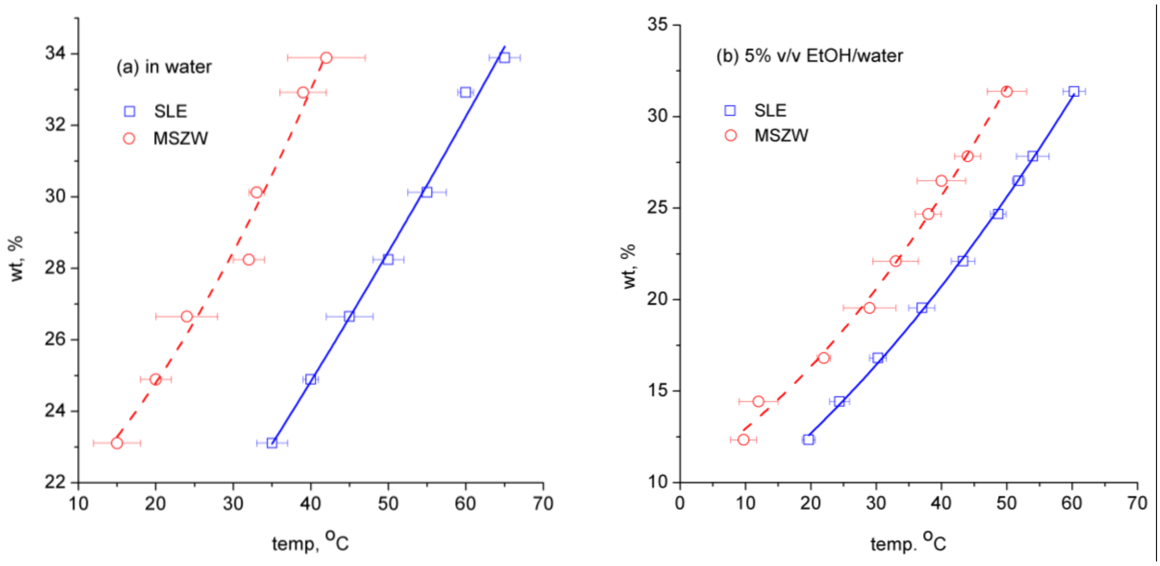

Figure 6. *SLE and MSZW in case of water (left) and mixed solvent (right)*

Saturated solutions at 60°C with two types of solvents, water and water containing 5% (v/v) ethanol, were cooled at a rate of 1°C.min^{-1}. The primary nucleation process was monitored using laser technology, which detected abrupt changes in the sample's transmittance. The term "cloud point" is used to describe this moment. The results are also presented in Figure 6, each measurement was repeated 5 times to take mean values.

In Figure 6a, the metastable zone boundary is parallel to the solubility curve. The width of the bounded region between these two curves is approximately 20°C, which is relatively wide and provides a favorable range for performing the crystallization process. Therefore, two crystallization operating modes were designed based on this boundary: deep cooling, which corresponds to conditions near the boundary, and moderate cooling, which occurs relatively farther from the MSZW boundary. The outcomes of these crystallization modes will be presented in the following section.

In contrast, when ethanol is present, the MSZW is significantly reduced, with its width narrowing to just 10°C as seen in Figure 6b. This creates a constrained operational region for conducting the crystallization process within this zone. However, operating in such a narrow range demands higher precision in process control. Special attention must be given to factors such as the nucleation rate and the resulting changes in crystal morphology under effects of ethanol.

3.4. Crystallization operation

3.4.1. Liquidus trajectory of different crystallization modes

Figure 7 presents the crystallization trajectories through changes in liquid-phase concentration. Overall, all crystallization processes are controlled within the MSZW, but each operational mode exhibits distinct characteristics.

In the deep cooling as mode #1, nucleation occurs rapidly, and the crystallization trajectory quickly approaches the liquid-solid equilibrium curve at 35°C. At this point, the driving force for crystallization, represented by the degree of supersaturation, reaches zero, and the crystallization process ceases.

In contrast, under the lower supersaturated level as mode #2, the crystallization trajectory also progresses toward the liquid-solid equilibrium but at a slower rate, as shown in Figure 7. This slower progression is expected to result in larger and more uniform crystals compared to the rapid cooling mode.

Notably, under the influence of ethanol, the crystallization trajectory proceeds very quickly. However, the resulting crystals are much smaller in size, reflecting the impact of ethanol on the crystallization dynamics.

Thus, alongside the changes in turbidity change of the liquid phase, the formation and evolution of the solid phase are of particular interest. In the following section, solid particle distribution will be analyzed over time, with a focus on the number of particle being in each population. This statistical approach aims to reveal the changes in the solid phase during the crystallization process.

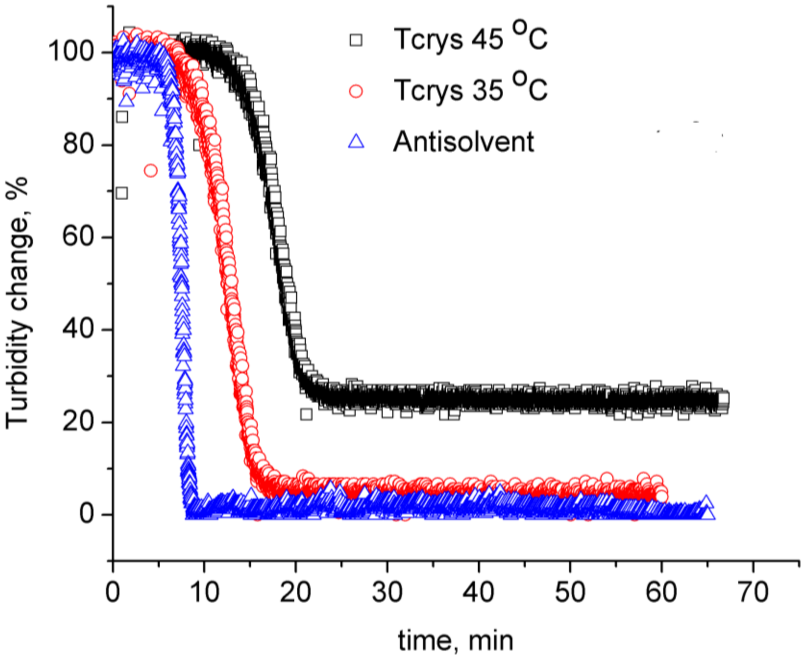

Figure 7. *Crystallization trajectory*

3.4.2. Solid evolution profiles

Mode #1: 20 °C of supercooling with water as solvent

Figure 8 illustrates the change in particle size distribution over time for the isothermal seeding crystallization mode, where a saturated system at 55°C is cooled to 35°C, corresponding to a 20°C supercooling. After nucleation, the equivalent distribution is represented for each time interval at 0, 5, 10, and 30 minutes. The quantity of solid phase obtained can be inferred from the decrease in the liquid phase based on the law of mass conservation.

Obviously, over time, the amount of solid phase will simply increase until the system reaching equilibrium. Therefore, a key focus of this study is the particle size distribution of the solid phase as it evolves. Understanding this distribution is crucial for optimizing crystal growth and ensuring desired particle size characteristics.

It is evident that from 0 to 5 minutes, the average crystal size increases only marginally, even though the liquid-phase curve indicates a sharp decrease in solute concentration. This suggests that during this period, secondary nucleation predominantly occurs due to the added seeds. Within a very short time, a large number of crystals are generated, but their small size results in a negligible increase in the average size.

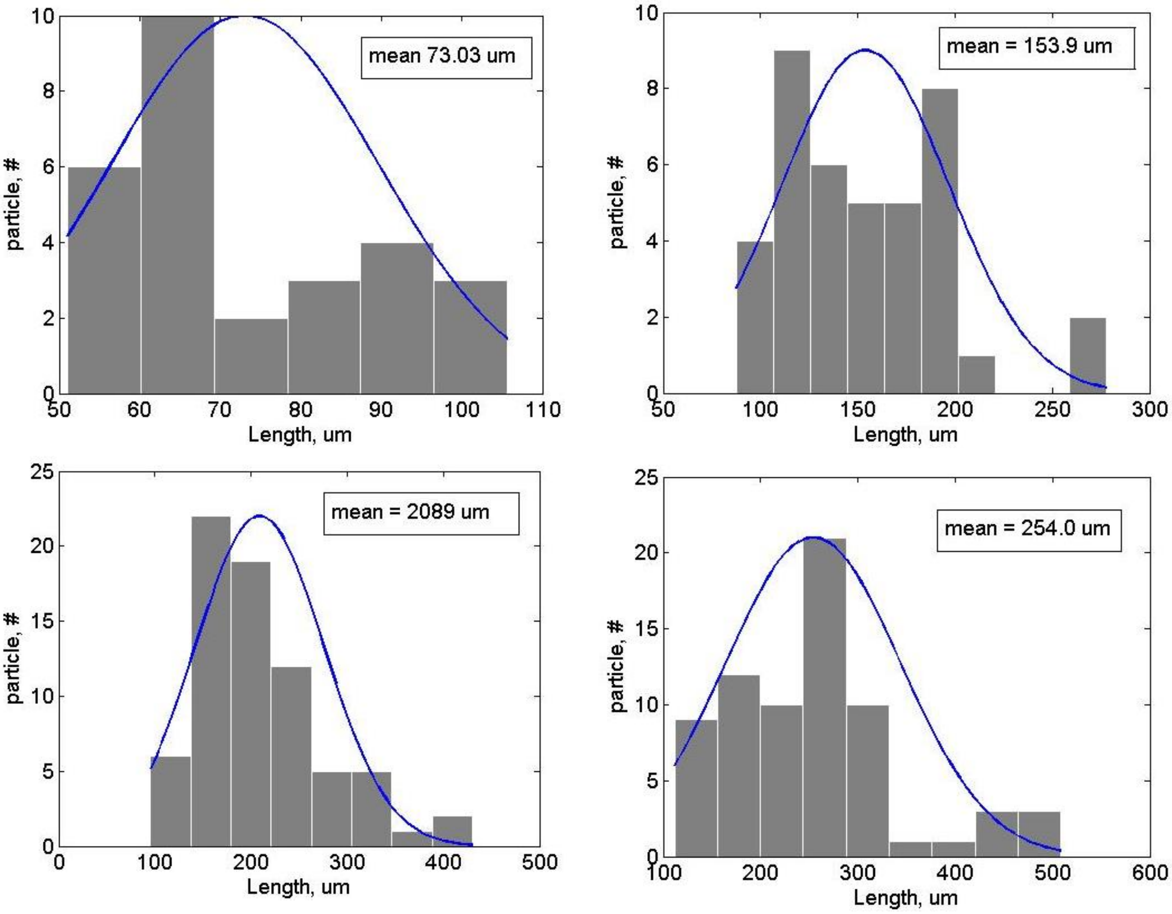

Figure 8. *PSD over time of Mode #1*

The particle size distribution (PSD) at 10 minutes reveals that during this phase, the crystals grow rapidly, reaching an average size of 208.9 microns. By 30 minutes, the crystals achieve an average size of 254.0 microns, demonstrating significant growth over time.

Mode #2: 10 ºC of supercooling in water as solvent

The second experiment followed a similar operational method to the first but maintained a lower degree of supercooling at 10°C instead of 20°C. After the seed formation, the system still underwent secondary nucleation, similar to the first case, causing the average particle size to increase from 99.6 to 189.7 µm. However, compared to the first experiment, this size increase occurred at a relatively slower rate.

This slower rate allowed the crystals sufficient time to grow into more complete and well-formed structures. Indeed, samples analyzed at 10 and 30 minutes showed that the average particle size increased to 335.4 and 342.3 µm, respectively. Thus, with a smaller degree of supercooling, the process favors crystal growth over the formation of new nuclei, resulting in more uniform and mature crystals.

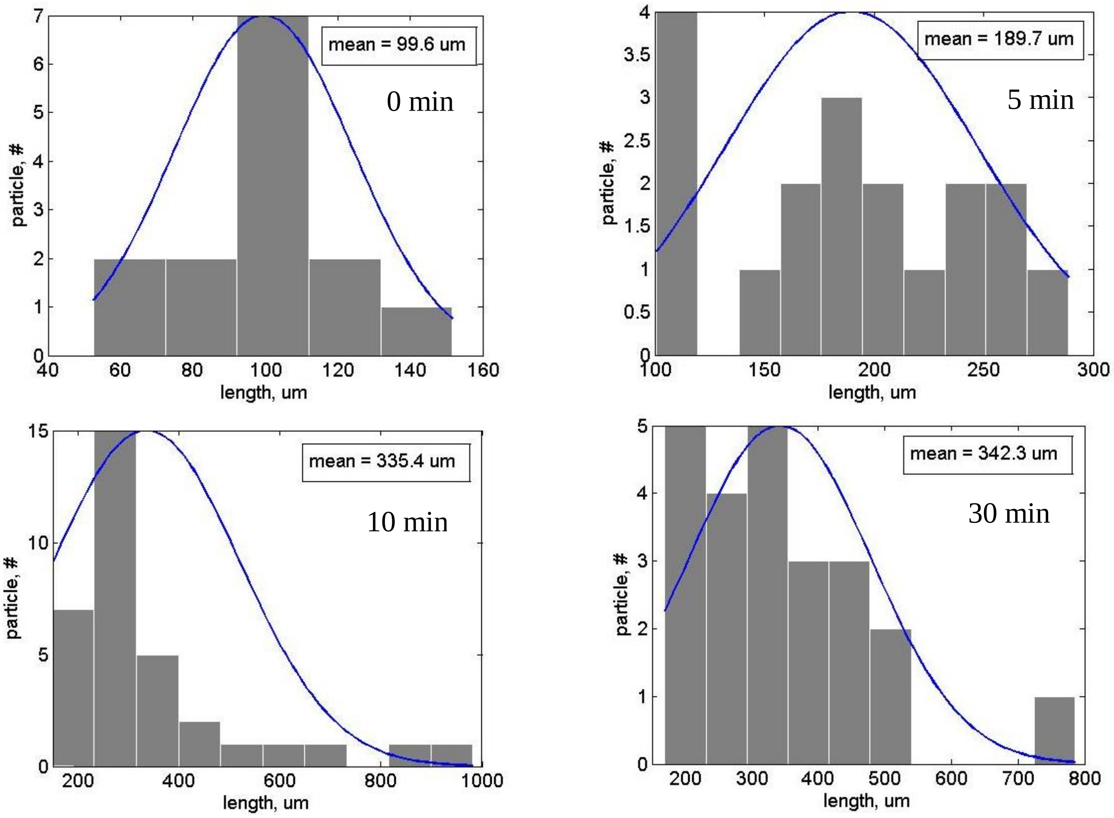

Figure 9. *PSD over time of Mode #2*

Mode #3: antisolvent crystallization

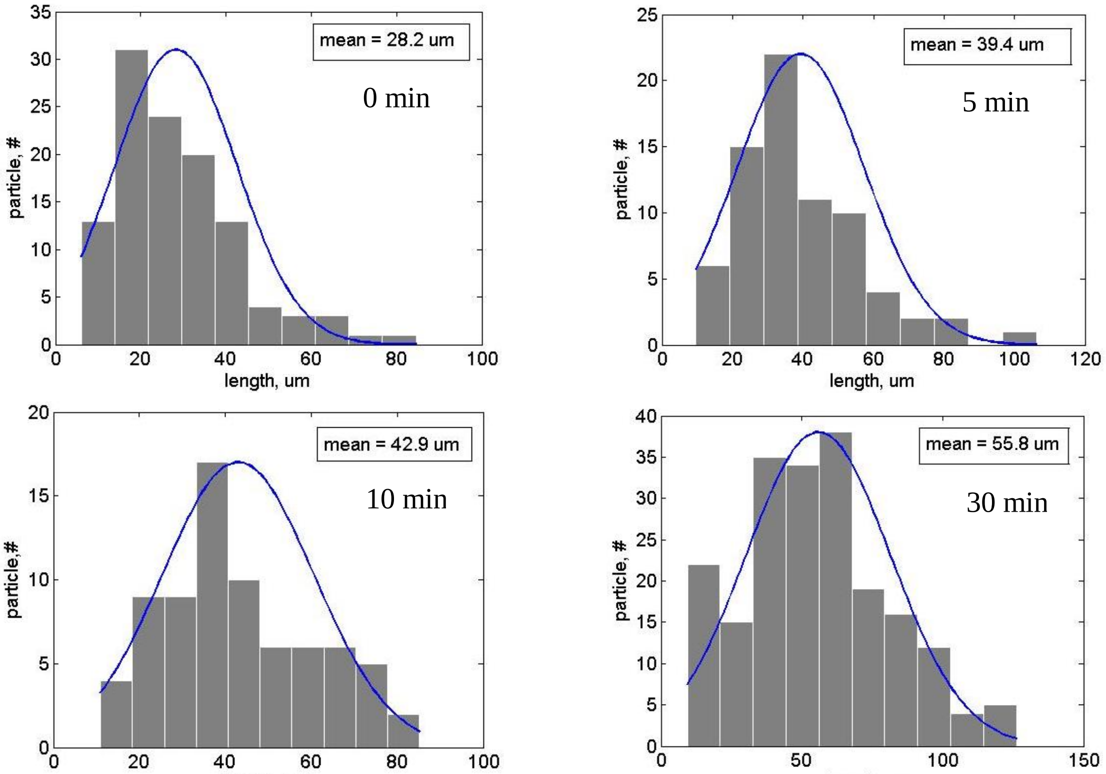

Figure 10. *PSD over time of Mode #3*

Figure 10 presents a PSD evolution profile for an antisolvent crystallization process. In this case, due to the very narrow MSZW, seeding is unnecessary. In practice, the addition of ethanol immediately induces rapid crystallization, as evidenced by the PSD at 0 and 5 minutes with small crystals.

This process involves spontaneous primary nucleation, resulting in highly uniform and small seed crystals. The PSD is distributed within a very narrow range. Data from subsequent time points, at 10 and 30 minutes, reveal that the crystal are much smaller than those in the first two cases, the system reach equilibrium with an equivalent diameter of 55.8 µm.

Thus, this third operating mode produces a product with entirely distinct characteristics, emphasizing the impact of antisolvent crystallization on particle size and distribution.

The results of the three crystallization operating modes are summarized in Table 1. Overall, the different crystallization modes play a decisive role in determining the properties of the final product.

Table 1. *PSD variation and product purity obtained from three operation modes*

	0 min	5 min	10 min	30 min	Purity (EDS.)
Mode #1	73.0 µm	153.9 µm	208.9µm	254.0 µm	98.1%
Mode #2	99.6 µm	189.7 µm	335.4 µm	342.3 µm	99.7%
Mode #3	28.2 µm	39.4 µm	42.9 µm	55.8 µm	96.2%

4. Conclusions

This paper presented a comprehensive study, encompassing investigations from the solid-phase structure to the thermodynamic properties of the liquid-solid equilibrium process. The solubility of KDP in water was found to be relatively high, while the addition of ethanol significantly reduced solubility, confirming ethanol's role as an antisolvent in the KDP-water system. However, KDP remains the same solid phase under studied conditions.

In addition to thermodynamics, kinetic phenomena were thoroughly investigated, including spontaneous nucleation processes and the determination of MSZW under various conditions. Based on the results, three crystallization modes were designed and operated, focusing on the roles of supersaturation and ethanol.

The experiments demonstrated that at a supersaturation level of 20°C, the resulting crystals were much smaller than those obtained at a supersaturation level of 10°C. Notably, when ethanol was introduced, the nucleation rate became dominant, surpassing the crystal growth rate, leading to the formation of very small crystals. PSD was found uniform and ranged from 20 to 120 µm.

In conclusion, different crystallization modes, if carefully controlled, can produce products with desired particle sizes tailored for various applications. Furthermore, the obtained data in this work provide opportunity for process modeling via e.g. Population Balance Method (PBE) since this method requires PSD data as critical input parameters.

Nomenclature

NaDP	sodium dihydrogen phosphate
KDP	potassium dihydrogen phosphate
MSZW	metastable zone width
NLO	nonlinear optical material
PSD	particle size distribution
PBE	Population Balance Method
SLE	solid-liquid-equilibria

Acknowledgments

The authors would like to thank supports from HCMUTE and students in the class EIE420103.

Conflict of Interest

The authors declare that there is no conflict of interest.

REFERENCES

[1] K. Jancaitiene, R. Šlinkšien, and R. Žvirdauskien, “Properties of potassium dihydrogen phosphate and its effects on plants and soil,” *Open Agric.*, vol. 8, p. 20220167, 2023.

[2] W. Hu, J. Wang, Q. Deng, D. Liang, H. Xia, L. Lin, and X. Lv, “Effects of different types of potassium fertilizers on nutrient uptake by grapevine,” *Horticulturae*, vol. 9, p. 470, 2023.

[3] L. Deng, J. Duan, X. Zeng, H. Yang, and S. Huang, “A study on dual laser beam separation technology of KDP crystal,” *Int. J. Mach. Tools Manuf.*, vol. 72, pp. 1–10, 2013.

[4] I. Pritula *et al.*, “Linear and nonlinear optical properties of dye-doped KDP crystals: Effect of thermal treatment,” *Opt. Commun.*, vol. 282, pp. 1141–1147, 2009.

[5] R. Raja, D. Vedhavalli, P. K. Nathan, and R. Kanimozhi, “Growth and characterization of KDP doped single crystal,” *Int. J. Mater. Sci.*, vol. 12, pp. 273–281, 2017.

[6] R. S. Priyadharshini and M. Saravanan, “Doped potassium dihydrogen phosphate single crystals with enhanced second-harmonic generation efficiency: An investigation of phase purity, nonlinear, piezoelectric, optical, and crystalline qualities,” *Phys. Scr.*, vol. 98, p. 025801, 2023.

[7] S. Lee, H. S. Wi, W. Jo, and J. Y. Cho, “Multiple pathways of crystal nucleation in an extremely supersaturated aqueous potassium dihydrogen phosphate (KDP) solution droplet,” *Proc. Natl. Acad. Sci. USA*, vol. 113, pp. 13618–13623, 2016.

[8] T. L. Minh, T. P. Thanh, N. N. T. Hong, and V. P. Minh, “A simple population balance model for crystallization of L-lactide in a mixture of n-hexane and tetrahydrofuran,” *Crystals*, vol. 12, p. 221, 2022.

[9] J. Nývlt, O. Söhnel, M. Matachová, and M. Broul, *The Kinetics of Industrial Crystallization*. Amsterdam, The Netherlands: Elsevier, 1985.

[10] T. M. Le, T. D. Nguyen, G. T. Nguyen, and N. T. Tran, “Antisolvent effects of C1–C4 primary alcohols on solid-liquid equilibria of potassium dihydrogen phosphate in aqueous solutions,” *ChemEngineering*, vol. 7, p. 99, 2023.

[11] P. A. Barata and M. L. Serrano, “Thermodynamic representation of the solubility for potassium dihydrogen phosphate (KDP) + water + alcohols systems,” *Fluid Phase Equilib.*, vol. 141, pp. 247–263, 1997.

[12] D. Chen, S. Zhang, J. Liu, C. Zha, and R. Pan, “Morphological analysis of KDP-crystal workpiece surfaces machined by ultra-precision fly cutting,” *Materials*, vol. 13, p. 432, 2020, doi: 10.3390/ma13020432.

[13] Syrris, “What is crystallization and what are the methods of crystallization?” [Online]. Available: https://www.syrris.com/applications/what-is-crystallization-and-what-are-the-methods-of-crystallization

[14] L. Tam, T. Phan, N. Nguyen, and D. Duong, “Application of the polythermal method in constructing a quick solid-liquid equilibrium determination of L-lactide in a solvent mixture of 40% mass percentage of n-hexane in tetrahydrofuran,” *VNUHCM J. Nat. Sci.*, vol. 5, pp. 1474–1481, 2021.

[15] T. L. Minh, V. T. T. Nhu, V. T. Nga, and H. M. Hao, “Investigation of thermodynamic equilibria of vitamin C in various solvents via experimental determination and model correlation,” *JTE*, vol. 70B, pp. 94–101, 2022.

[16] T. M. Le, N. Y. Bui, and D. N. Tan, “In-situ and in real-time observation of particulate processes in lactic fermentation,” *TNU J. Sci. Technol.*, vol. 6, p. 229, 2024, doi: 10.34238/tnu-jst.10020.

[17] T. L. Minh, *Designing Crystallization-Based Enantiomeric Separation for Chiral Compound-Forming Systems in Consideration of Polymorphism and Solvate Formation*. Dr Hut Publisher, 2013. ISBN: 978-3-8439-1562-5.

[18] L. A. Bromley, “Thermodynamic properties of strong electrolytes in aqueous solutions,” *AIChE J.*, vol. 19, pp. 313–320, 1973.

Le Minh Tam, PhD at Max Planck Institute for Dynamics of Complex Technical Systems, Magdeburg, Germany. Postdoctoral research at Vietnam Academy of Science and Technology. Editorial Board Member of JCERU journal. Expertise in the fields of advanced materials, enantiomer separation, crystallization, chromatography, process analytical technology (PAT), chemical and bio-process engineering.

Email address: tamlm@hcmute.edu.vn. ORCID: https://orcid.org/0000-0002-5372-346X

Bui Thi Thanh Phuong received bachelor’s degree in food technology at Nong Lam University, Ho Chi Minh City, Viet Nam in 2015. In 2015, Phuong conducted a research project to create a syrup with high vitamin C content extracted from Acerola. Phuong is currently pursuing a master’s degree for Food Technology at Nong Lam University. Email address: Thanhphuongbui71@gmail.com. ORCID: https://orcid.org/0009-0006-0791-6750

Associate Professor Kha Chan Tuyen is currently Head of Department of Food Microbiology and Product Development and Acting Dean of the Faculty of Chemical Engineering and Food Technology, Nong Lam University, Ho Chi Minh City, Viet Nam. Kha’s research interest focuses on extraction and encapsulation of bioactive compounds, and thermal processes. He has authored over 70 scientific publications, including peer-reviewed papers and refereed proceedings, 02 reference books, 01 edited book, 05 book chapters, and participated in various national and international conferences, seminars and workshops. Since 2017, he has been appointed as a coordinator of Better Process Control School in collaboration with FDA and CBA (United States). Email address: khachantuyen@hcmuaf.edu.vn. ORCID: https://orcid.org/0000-0003-0632-7197